

# Narrow-width approximation limitations

N. Kauer

*Institut für Theoretische Physik, Universität Würzburg, D-97074 Würzburg, Germany*

(Dated: February 2, 2008)

The quality of the narrow-width approximation is examined for partonic and convolved cross sections of sample processes. By comparison with accurate predictions significant limitations are revealed.

PACS numbers: 25.75.Dw, 11.80.Fv, 12.60.-i

The narrow-width approximation (NWA) is widely applied to predict the probability for resonant scattering processes when the total decay width  $\Gamma$  of the resonant particle is much smaller than its mass  $M$ . In the limit  $\Gamma \rightarrow 0$ , the squared propagator  $D(q^2) \equiv \left[ (q^2 - M^2)^2 + (M\Gamma)^2 \right]^{-1}$  with 4-momentum  $q$  approaches  $D(q^2) \sim K\delta(q^2 - M^2)$  with  $K = \pi/(M\Gamma) = \int_{-\infty}^{\infty} dq^2 D(q^2)$ . The scattering cross section  $\sigma$  thus approximately decouples into on-shell production ( $\sigma_p$ ) and decay as shown in Eq. (1) for a scalar process [1]. The generalization to multiple resonances is straightforward.

We use the notation of [2], Sec. 38. Based on the scales occurring in  $D(q^2)$ , the conventional error estimate is  $\mathcal{O}(\Gamma/M)$ . The branching fraction for the considered decay mode is then given by  $\text{BR} = \Gamma_X/\Gamma = \sigma_{\text{NWA}}/\sigma_p$ , where  $\Gamma_X$  is the partial decay width. We define the effective branching ratio  $\text{BR}_{\text{eff}} \equiv \sigma/\sigma_p$ , which is related to the branching ratio via  $\text{BR}_{\text{eff}} = (1 + R)\text{BR}$  with  $R \equiv \sigma/\sigma_{\text{NWA}} - 1 = R^{(1)} + \mathcal{O}(\Gamma^2)$ .

To examine the conventional error estimate, we calculate  $R^{(1)}$  for the scalar process of Fig. 1. Here,  $|\mathcal{M}_p|^2 \propto 1/(t - m_p^2)^2$  [3] and  $|\mathcal{M}_d|^2 \propto 1$ .

$$\sigma = \frac{(2\pi)^7}{2s} \int_{q_{\min}^2}^{q_{\max}^2} dq^2 \int d\phi_p |\mathcal{M}_p(q^2)|^2 D(q^2) \int d\phi_d |\mathcal{M}_d(q^2)|^2 \approx \sigma_{\text{NWA}} \equiv \frac{(2\pi)^7}{2s} \int d\phi_p |\mathcal{M}_p(M^2)|^2 K \int d\phi_d |\mathcal{M}_d(M^2)|^2 \quad (1)$$

$$R^{(1)} = \left\{ \frac{M(s - m_d^2)}{\pi(m_d^2 - M^2)(s - M^2)} + [\pi M(m_d^2 - M^2)(s - M^2)(s + m_p^2)(s - M^2 + m_p^2)]^{-1} \left[ m_d^2 s (s - M^2 + m_p^2)^2 \ln \frac{s}{m_d^2} + (s + m_p^2) \left( m_d^2 (s(s + m_p^2) - 2M^2 s + M^4) - M^4 m_p^2 \right) \ln \frac{M^2 - m_d^2}{s - M^2} + M^4 m_p^2 (s - m_d^2 + m_p^2) \ln \frac{s - m_d^2 + m_p^2}{m_p^2} \right] \right\} \cdot \Gamma \quad (2)$$

The result in Eq. (2) shows that  $R$  and hence  $\text{BR}_{\text{eff}}$  depend not only on  $\Gamma$  and  $M$ , but on additional scales introduced through the center of mass energy  $\sqrt{s}$  or particle masses in production or decay. Selection cuts have a similar impact that is not explicitly considered here. Note that the actual relative deviation in units of the conventionally expected error, i.e.  $R/(\Gamma/M)$ , is width independent to first approximation in  $\Gamma$ . As the threshold  $\sqrt{s} = M$  is approached the on-shell production phase space volume vanishes and  $\sigma_{\text{NWA}} \rightarrow 0$  while  $\sigma$  remains finite.  $R$ , hence, diverges and the NWA becomes unreliable. From Eq. (2) one also sees that  $R$  diverges in the limit  $m_d \rightarrow M$ , i.e. when the sum of the daughter masses approaches the mass of the decaying particle. The NWA can thus not be used for all decay modes in scenarios with almost degenerate mass hierarchies. We illustrate the behaviour of  $R$  in Fig. 2. For  $m_d \lesssim 0.9M$  and  $\sqrt{s} \gtrsim 1.1M$ ,

the NWA uncertainty is indeed of  $\mathcal{O}(\Gamma/M)$ . Note that while  $R/(\Gamma/M) \lesssim -10$  for  $\sqrt{s} \gtrsim 1.01M$ , it turns positive for yet smaller values of  $\sqrt{s}$  (see also Fig. 4). The  $m_p$ -dependence of the ratio  $R$  is in general relatively weak despite the mass singularity in the production cross section. We note that significant deviations in the threshold region have been observed in connection with Standard Model (SM) predictions for  $W$ -pair production and decay in  $e^+e^-$  collisions [4].

Resonant cross sections typically peak just above threshold. In Figs. 3 and 4, we illustrate the accuracy of the NWA above threshold for reactions with distributed  $\sqrt{s}$  by displaying  $\tilde{\sigma}_{[\text{NWA}]}(\sqrt{\hat{s}_{\max}}) \propto 1/s \int_0^{\hat{s}_{\max}} d\hat{s} \sigma_{[\text{NWA}]}(\hat{s}) \ln(s/\hat{s})$  corresponding to constant incoming particle (parton) momentum distribution functions (PDFs) and  $\tilde{R} \equiv \tilde{\sigma}/\tilde{\sigma}_{\text{NWA}} - 1$  normalized to  $\Gamma/M$ .

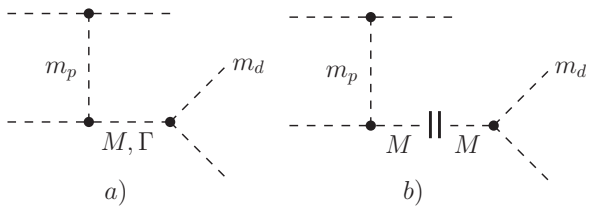


FIG. 1: Scalar process with (a) Breit-Wigner propagator and (b) in NWA. The double bars indicate the decoupling of production and decay. Lines without labels correspond to massless particles.

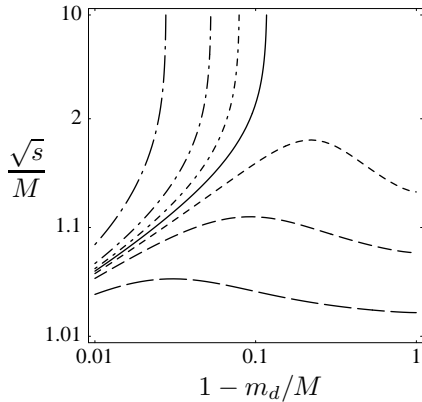


FIG. 2: Contour plot of  $R \equiv \sigma/\sigma_{\text{NWA}} - 1$  normalized to  $\Gamma/M = 0.01$  as function of  $\sqrt{s}$  and  $m_d$  for the process of Fig. 1 with  $m_p = 0.02 M$ . Contour lines are shown for  $R = 0$  (solid),  $R > 0$  (dot-dashed) and  $R < 0$  (dashed) with  $|R|/(\Gamma/M) \in \{1, 3, 10\}$ . The dash length increases with magnitude.

Like  $R/(\Gamma/M)$ ,  $\tilde{R}/(\Gamma/M)$  does not depend on  $\Gamma/M$  in first approximation. At hadron colliders, the convolution with steeply falling PDFs enhances the weight of the region around and below threshold. It also affects the resonance line shape, i.e. alters the  $d\sigma/dq^2$  distribution, whereas in NWA the Breit-Wigner is integrated out unmodified into  $K$ .

Next, we consider a process with non-scalar particles and more complex interactions. More specifically, we repeat our analysis for the process in Fig. 5. Here,  $|\mathcal{M}_p|^2 \propto (t + 2s - q^2)^2/(t - m_p^2)^2$  and  $\sum_{\text{spin}} |\mathcal{M}_d|^2 \propto q^2 - m_d^2$ . For this process, the  $\mathcal{O}(\Gamma)$ -result for  $R$  corresponding to Eq. (2) contains dilogarithms and is too complex to be displayed here. Fig. 6 shows that for this process comparable enhancements occur already at less extreme parameter values. As shown in Fig. 7, the large off-shell increase for higher  $\sqrt{s}$  leads to a continued rise of  $\tilde{R}$  for constant PDFs. With the steeply falling PDFs characteristic for hadron colliders, however, the ratio saturates as seen in Fig. 8 for  $\tilde{\sigma}'_{[\text{NWA}]}(\sqrt{\hat{s}_{\text{max}}}) \propto 1/s \int_0^{\hat{s}_{\text{max}}} d\hat{s} \sigma_{[\text{NWA}]}(\hat{s}) \int_{\hat{s}/s}^1 dx/x f(x) f(\hat{s}/(xs))$  with  $f(x) \propto (1-x)^9/\sqrt{x}$ .

In addition to resonant amplitudes, typically nonresonant or subresonant amplitudes contribute, too, but are

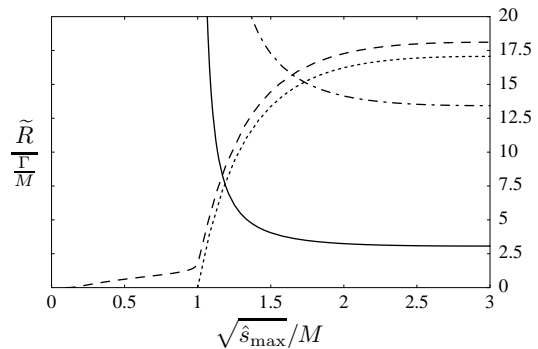


FIG. 3: The cross sections  $\tilde{\sigma}$  (dashed) and  $\tilde{\sigma}_{\text{NWA}}$  (dotted) in unspecified normalization and  $\tilde{R} \equiv \tilde{\sigma}/\tilde{\sigma}_{\text{NWA}} - 1$  normalized to  $\Gamma/M$  (solid) are shown as functions of  $\sqrt{\hat{s}_{\text{max}}}$  (see main text) for the process of Fig. 1 with  $\Gamma = 0.02 M$ ,  $m_p = 0.01 M$ ,  $m_d = 0.1 M$  and  $\sqrt{s} = 3 M$ .  $\tilde{R}/(\Gamma/M)$  with  $m_d = 0.001 M$  is also displayed (dot-dashed).

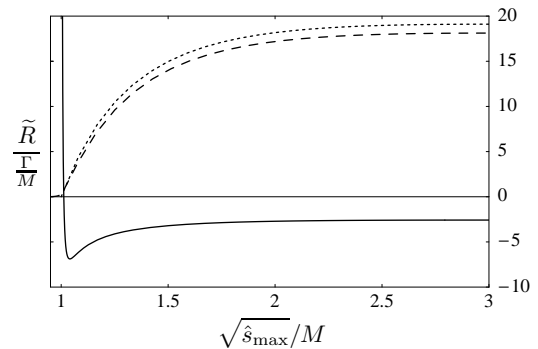


FIG. 4: The cross sections  $\tilde{\sigma}$  and  $\tilde{\sigma}_{\text{NWA}}$  as well as  $\tilde{R}$  are shown for the process of Fig. 1 with  $m_d = 0.9 M$ . Other details as in Fig. 3.

expected to be suppressed. We discuss the effect of these contributions by means of the scattering of a massless fermion with electric charge  $Q_f = 0$  and a longitudinally polarized  $W^-$  boson in the GWS model (see [5] and [2], Sec. 10). The contributing Feynman graphs are shown (and our notation is clarified) in Fig. 9. The corresponding amplitudes are given by  $\mathcal{M}_s = \mathcal{C} \cdot s/m^2/(s - M^2 + iM\Gamma)$  and  $\mathcal{M}_t = \mathcal{C} \cdot (2 - (s - 3m^2)(s + m^2)t/m^2/(s - m^2)^2)/(t - m_Z^2)$  with  $\mathcal{C} = -ig^2/2\sqrt{(s - m^2)^2 + st}$ , where  $g$  is the weak coupling constant. Close to resonance, the

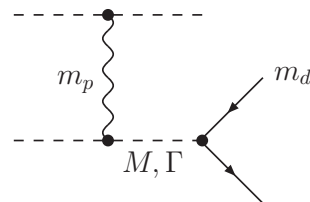


FIG. 5: Process with non-scalar particles in production (gauge vector boson) and decay (fermions).

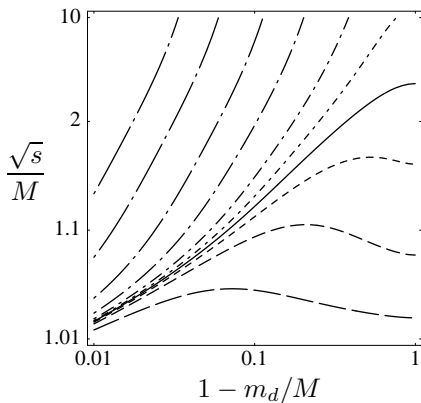


FIG. 6: Contour plot of  $R$  as function of  $\sqrt{s}$  and  $m_d$  for the process of Fig. 5. Contour lines for  $R/(\Gamma/M) \in \{-10, -3, -1, 0, 1, 3, 10, 30, 100, 300\}$  are shown. Other details as in Fig. 2.

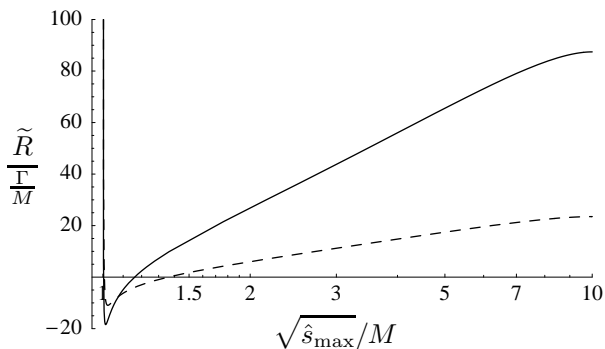


FIG. 7:  $\tilde{R}$  is shown as function of  $\sqrt{\hat{s}_{\max}}$  for the process of Fig. 5 with  $m_d = 0.95M$  (solid) and  $m_d = 0.9M$  (dashed) for  $\sqrt{s} = 10M$ . Other details as in Fig. 3.

$\mathcal{M}_s$  contribution is expected to exceed the  $\mathcal{M}_t$  contribution by  $\mathcal{O}((M/\Gamma)^2)$ . In our example with a neutral external fermion this is indeed the case. For  $|Q_f| \neq 0$ , however, the additional graph with  $t$ -channel exchange of a massless photon will make the nonresonant contribution divergent in the zero-mass limit for the external fermion, while the resonant and  $Z$ -exchange contributions do not diverge for finite  $m$ . Nonresonant contributions can thus be larger than anticipated. After integrating the Breit-Wigner a resonant enhancement of the cross section by  $\mathcal{O}(M/\Gamma)$  is expected. This requires that the contribution from resonant graphs has to dominate not only close to resonance, but also in the region with  $|\sqrt{s} - M| \gtrsim \Gamma$ , which contributes 30% even when nonresonant graphs are negligible. If the affected phase space regions can be distinguished and eliminated experimentally, these effects can be suppressed. We note that a significant impact of sub- and nonresonant contributions has been observed for  $W$  boson [6] and top quark [7] production and decay in the SM.

For processes with significant nonresonant amplitude ( $\mathcal{M}_{nr}$ ) contribution one could apply the NWA to the res-

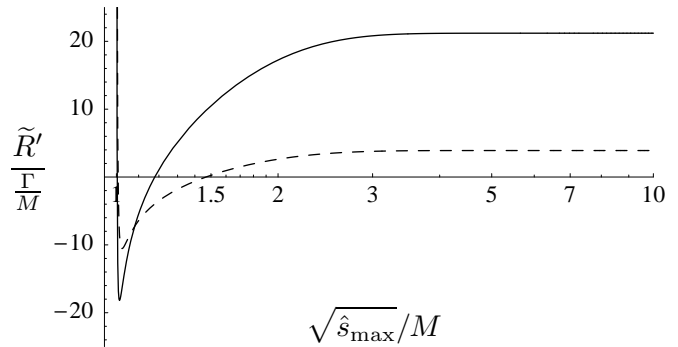


FIG. 8:  $\tilde{R}' \equiv \tilde{\sigma}'/\tilde{\sigma}'_{\text{NWA}} - 1$  with cross sections  $\tilde{\sigma}'$  and  $\tilde{\sigma}'_{\text{NWA}}$  that involve steeply falling PDFs (see main text) is shown as function of  $\sqrt{\hat{s}_{\max}}$  for the process of Fig. 5 with  $m_d = 0.95M$  (solid) and  $m_d = 0.9M$  (dashed) for  $\sqrt{s} = 10M$ . Other details as in Fig. 3.

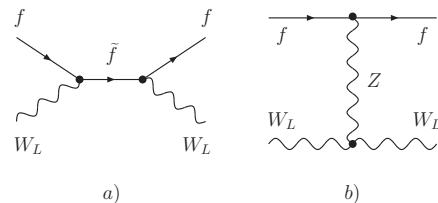


FIG. 9: Scattering of a massless, neutral fermion and a longitudinally polarized  $W^-$  boson in the GWS model with (a)  $s$ -channel ( $\mathcal{M}_s$ ) and (b)  $t$ -channel ( $\mathcal{M}_t$ ) amplitude contributions. For  $\sqrt{s} \approx m_{\tilde{f}} \equiv M > m_W \equiv m$  the  $s$ -channel contribution will be resonant ( $\Gamma_{\tilde{f}} \equiv \Gamma$ ). The  $t$ -channel contribution with  $m_Z = m/\cos\theta_W$  is nonresonant.

onant amplitude ( $\mathcal{M}_r$ ) contribution and separately calculate and analyze the  $\mathcal{M}_{nr}$  contribution after one has established that the interference between both is negligible [8]. Fig. 10 exemplifies that  $\mathcal{M}_r$ - $\mathcal{M}_{nr}$  interference effects can be larger than the expected NWA uncertainty, even close to resonance. Note that the interference contribution can not be calculated in NWA, because then  $\mathcal{M}_r$  would have to be integrated with the on-, but  $\mathcal{M}_{nr}$  with the off-shell phase space. More accurate calculations that do not rely on the NWA are therefore always necessary to assess interference effects.

Having established various limitations of the NWA by considering selected examples, we conclude that more detailed studies for phenomenologically relevant processes are necessary to guarantee accurate predictions. We have investigated the quality of the NWA in the Minimal Supersymmetric Standard Model and find inaccuracies for relevant processes in not-ruled-out scenarios that are an order of magnitude larger than the conventional uncertainty estimate  $\mathcal{O}(\Gamma/M)$  of typically 1-10% [9]. This study also shows that secondary decays in cascades do in general not mitigate the deviation and in selected scenarios enhance it even further.

Beyond leading order, at least QCD corrections should be taken into account since they are generally of similar

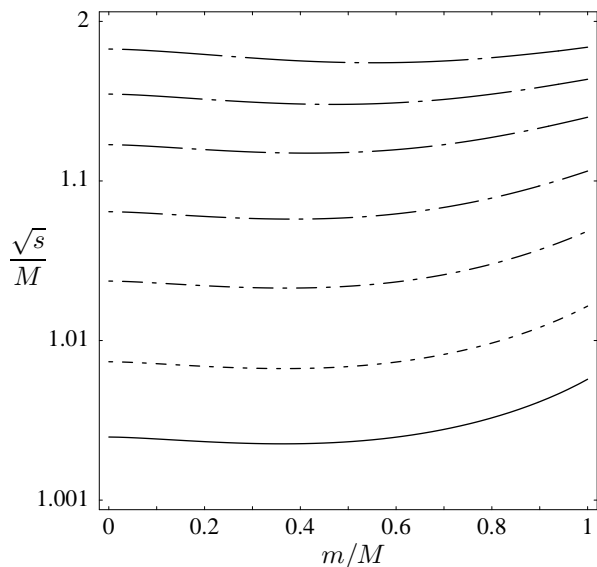


FIG. 10: Contour plot of  $R_i \equiv (\sigma(\mathcal{M}_s) + \sigma(\mathcal{M}_t))/\sigma(\mathcal{M}_s + \mathcal{M}_t) - 1$  normalized to  $\Gamma/M = 0.01$  with the resonant  $s$ - and nonresonant  $t$ -channel cross section contributions for the process of Fig. 9 as function of the invariant mass of the resonant particle  $\sqrt{s}$  and  $W$  mass  $m$  for  $\cos\theta_W = 0.8$ . Contour lines are shown for  $R_i/(\Gamma/M) = 1$  (solid) and  $R_i/(\Gamma/M) \in \{3, 10, 30, 100, 300, 1000\}$  (dot-dashed). The dash length increases with magnitude.

### Acknowledgments

We would like to thank S. Dittmaier for useful comments after carefully reviewing the manuscript, as well as D. Berdine and D. Rainwater for numerous useful discussions. This work was supported by the BMBF, Germany (contract 05HT1WWA2).

- 
- [1] For unstable particles with spin,  $\sigma_{\text{NWA}} = \sigma_p \cdot \text{BR} +$  corrections if spin correlations are not neglected as seen explicitly after a Fierz transformation.
- [2] W. M. Yao *et al.* [Particle Data Group], *J. Phys. G* **33** (2006) 1.
- [3]  $t$  is defined with the two uppermost external momenta in all graphs.
- [4] W. Beenakker *et al.*, arXiv:hep-ph/9602351; W. Beenakker, F. A. Berends and A. P. Chapovsky, *Nucl. Phys. B* **548** (1999) 3 [arXiv:hep-ph/9811481].
- [5] S. L. Glashow, *Nucl. Phys.* **22** (1961) 579; S. Weinberg, *Phys. Rev. Lett.* **19** (1967) 1264; A. Salam, in *Elementary Particle Theory: Relativistic Groups and Analyticity (Nobel Symposium No. 8)*, edited by N. Svartholm (Almqvist and Wiksell, Stockholm, 1968), p. 367.
- [6] S. Dittmaier and M. Kramer, *Phys. Rev. D* **65** (2002) 073007 [arXiv:hep-ph/0109062]; U. Baur and D. Wackerth, *Phys. Rev. D* **70** (2004) 073015 [arXiv:hep-ph/0405191]; A. Denner, S. Dittmaier, M. Roth and L. H. Wieders, *Phys. Lett. B* **612** (2005) 223 [arXiv:hep-ph/0502063].
- [7] F. Gangemi, G. Montagna, M. Moretti, O. Nicrosini and F. Piccinini, *Nucl. Phys. B* **559** (1999) 3 [arXiv:hep-ph/9905271]; J. van der Heide, E. Laenen, L. Phaf and S. Weinzierl, *Phys. Rev. D* **62** (2000) 074025 [arXiv:hep-ph/0003318]; N. Kauer and D. Zeppenfeld, *Phys. Rev. D* **65** (2002) 014021 [arXiv:hep-ph/0107181]; K. Kolodziej, *Eur. Phys. J. C* **23** (2002) 471 [arXiv:hep-ph/0110063]; N. Kauer, *Phys. Rev. D* **67** (2003) 054013 [arXiv:hep-ph/0212091].
- [8] In general, a suitable gauge has to be chosen and applied throughout.
- [9] D. Berdine, N. Kauer and D. Rainwater, arXiv:hep-ph/0703058; D. Berdine, N. Kauer and D. Rainwater, in preparation.
- [10] C. Buttar *et al.*, arXiv:hep-ph/0604120.
- [11] R. G. Stuart, *Phys. Lett. B* **262** (1991) 113; A. Aeppli, G. J. van Oldenborgh and D. Wyler, *Nucl. Phys. B* **428** (1994) 126 [arXiv:hep-ph/9312212].
- [12] A. Denner, S. Dittmaier, M. Roth and D. Wackerth, *Nucl. Phys. B* **560** (1999) 33 [arXiv:hep-ph/9904472]; A. Denner, S. Dittmaier, M. Roth and L. H. Wieders, *Nucl. Phys. B* **724** (2005) 247 [arXiv:hep-ph/0505042].
- [13] A. P. Chapovsky, V. A. Khoze, A. Signer and W. J. Stirling, *Nucl. Phys. B* **621** (2002) 257 [arXiv:hep-ph/0108190]; M. Beneke, A. P. Chapovsky, A. Signer and G. Zanderighi, *Phys. Rev. Lett.* **93** (2004) 011602 [arXiv:hep-ph/0312331]; M. Beneke, A. P. Chapovsky, A. Signer and G. Zanderighi, *Nucl. Phys. B* **686** (2004) 205 [arXiv:hep-ph/0401002].
- [14] K. Melnikov and O. I. Yakovlev, *Phys. Lett. B* **324** (1994) 217 [arXiv:hep-ph/9302311]; V. S. Fadin, V. A. Khoze and A. D. Martin, *Phys. Rev. D* **49** (1994) 2247.